2021 43rd Annual International Conference of the
IEEE Engineering in Medicine & Biology Society (EMBC)
Oct 31 - Nov 4, 2021. Virtual Conference

A novel wrist rehabilitation exoskeleton using 3D-printed multi-segment mechanism

Shiqi Yang, Min Li, Jiale Wang, Tianci Wang, Ziting Liang, Bo He, Jun Xie, and Guanghua Xu

Abstract—Wrist rehabilitation exoskeleton can effectively assist wrist recovery from stroke. However, current wrist rehabilitation devices have shortcomings such as heavy weight, uncertain motion trajectory, etc. This paper proposes a wrist rehabilitation robot driven by 3D-printed multi-segment mechanism to realize wrist rehabilitation in three degrees of freedom. We conducted three tests including bearing force, rehabilitation trajectory, range of motion tests. The results prove this exoskeleton can provide enough force and torque, and it can achieve larger range of motion within the same motor displacement, that makes it more compact and lighter in hardware and less expensive in cost. Moreover, its motion trajectory can be controlled and stable, that makes it more applicable for real application in human rehabilitation.

***Clinical Relevance*— Stroke is the leading cause of hemiplegia, and this symptom usually degrades patients' living standard and flexibility. This device can offer patients stable wrist rehabilitation training in three degrees of freedom with compact and lightweight characteristics.**

I. Introduction

Wrist rehabilitation robots can be used as an effective and practical tool to assist wrist rehabilitation from stroke. Many different types of wrist exoskeletons have been designed in recent years. For instance, Gupta et al. [1] developed a rigid wrist rehabilitation exoskeleton with kinesthetic feedback. But given its rigid structure, it is bulky and not portable. Higuma et al. [2] designed a soft wrist rehabilitation exoskeleton that used spring blades to fulfill wrist movements in two degrees of freedom (DOFs). In this design, two spring blades are actuated by two linear motors, respectively. As regard of advantages, it realizes soft-rigid combination as well as compact and light requirements. But the device cannot move in a certain trajectory stably. Choi et al. [3] made a soft cable-driven wrist-wearable robot which could assist wrist to throw darts. Although soft structure is pretty flexible and safe for users, the robustness and driving force requirements are difficult to meet. Zhu et al. [4] designed a multi-segment mechanism to assist fingers moving stably in a bionic trajectory.

In summary, current wrist rehabilitation devices have several shortcomings, such as the contradiction between flexibility and robustness, the heavy weight caused by rigid structures, and the uncertain motion trajectory because of soft exoskeleton. When assisted by exoskeleton, if the rotation center of exoskeleton differs considerably from that of human wrist, a secondary injury may occur [2]. As regard of this, stable and suitable trajectory is needed in rehabilitation training. Furthermore, wrist has three DOFs, but most wrist rehabilitation exoskeleton can only perform two DOFs training.

In this paper, we propose a wrist rehabilitation robot driven by a 3D-printed multi-segment mechanism to solve the problems above. It is designed to realize flexible and various rehabilitation motion in three DOFs for the patients with wrist dysfunction. It can assist users fulfilling wrist motion such as flexion/extension, radial deviation/ulnar deviation, and pronation/supination. More importantly, the wrist exoskeleton can achieve the same range of motion with smaller motor displacement than the previous design[5]. Switching to smaller motors considerably reduces the weight and cost. Validation experiments are shown in part III to evaluate the range of motion, force characteristics, and motion trajectory .

II. Wrist Exoskeleton Mechanism

A. Requirements of design

Wrist's motions can be summarized as flexion/extension, radial deviation/ulnar deviation, and pronation/supination. Generally, the normal ranges of these motions are 75°/65°, 20°/30°, 70°/75°, respectively [5]. Our expectation is to design a rigid-soft combined wrist exoskeleton with three DOFs to fulfill these motions.

In our previous research, we utilized a wrist rehabilitation robot which was actuated by two linear motors with maximum stroke at 100 mm [5]. In this paper, wrist is assisted by sliding springs, but as the deformation of sliding spring is not limited, not only the motor displacement is not effectively used, but also the trajectory is unstable and uncontrollable. Most importantly, it can not realize three DOFs motion, so that it not applicable for complete wrist rehabilitation.

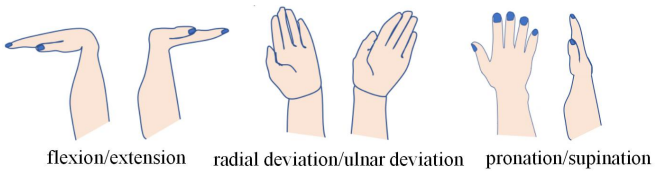

Figure 1. Three DOFs of motion in human wrist

In terms of rehabilitation requirements in wrist, Ryu et al. [6] studied the functional movements of the wrist joint and measured the normal angle of wrist movements. And the study by Lannin et al. [7] found that after a stroke, the muscles of patients with a stroke will reduce the range of joint motion by about 1/3 due to spasm and stiffness. In summary, the ranges of motions for wrist rehabilitation are set at 52°/45°, 15°/20°, 49°/52° for flexion/extension, radial deviation/ulnar deviation, and pronation/supination, respectively. According to the study of Japanese elderly [8], the average torque for wrist flexion and extension is 0.52Nm, and the velocity should not be strictly limited but compliant with safety and comfort considerations.

B. Overview of exoskeleton

Function of the exoskeleton is realized by an actuating unit including multi-segment mechanism and linear motor. As illustrated in Figure 2, when the two motors push the sliding springs, force will be transmitted to the hand plate that will bend the wrist. In contrast, there will be a reverse bend if the motors pull the springs. However, if they act differently the wrist will fulfill pronation or supination (see *Section D*). Apart from these, user's wrist can realize ulnar deviation and radial deviation when one motor maintains the temporal displacement and another pulls.

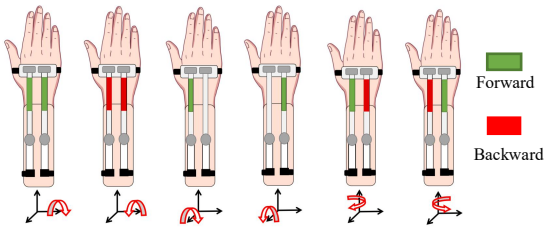

Figure 2. Wrist motion with different motor actions

Specifically, the multi-segment mechanism's design is shown in Figure 3. The last block was fixed on the end of the sliding spring, and each of them is separately sewn on the bottom cloth which is not elastic. These blocks have a through-hole, by which they are threaded and assembled together on a sliding spring. The end point of the mechanism is mounted on the hand plate by bearings, this design is to transmit the input linear force into wrist torque. That scenario is illustrated in Figure 3 (a) , and Figure 4 explains the realization process of pronation and supination.

C. Design of wrist-oriented multi-segment mechanism

The principle diagram is shown in Figure 3 (a), during flexion of the wrist, assuming the arc length of the sliding spring is L_1 the total length of the mechanism at the wrist joint is l, motor stroke is S_1. The distance from the sliding spring to the wrist is H whose value is the distance from the sliding spring to the bottom of the blocks (h) pluses the distance from the bottom of the sliding spring to the watch face (H_0). θ is the wrist rotation angle during flexion, R_1 is the bending radius. According to geometric relation, the following formats can be induced.

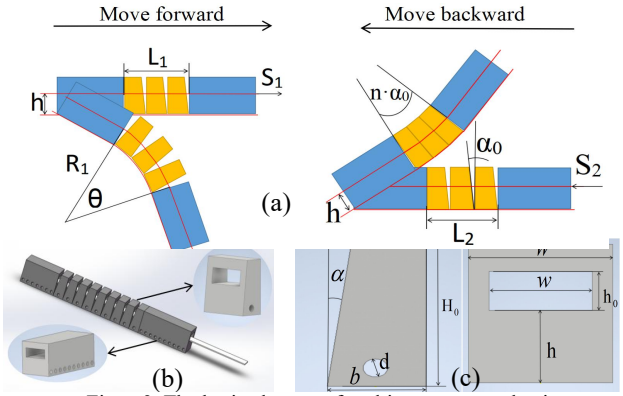

Figure3. The basic element of multi-segment mechanism

$$L_1 - l = S \tag{1}$$

$$R_1 = \frac{l}{2\tan\frac{\theta}{2}} + H \tag{2}$$

$$S_1 = \left(\frac{l}{2\tan\frac{\theta}{2}} + H \right) \cdot \theta - l \tag{3}$$

Similarly, when wrist stretches, the wrist rotation angle during flexion is $n \cdot \alpha_0$, the number of multi-segment blocks in wrist joint is n, angles between these blocks is α_0, arc length of the sliding spring is L_2. The total length of the multi-segment blocks at the wrist joint is l, motor drawback displacement is S_2. Consequently, the geometric relation of extension is established.

$$S_2 = l - \left(\frac{l}{2tan(\frac{n \cdot \alpha_0}{2})} - h \right) \cdot n\alpha_0 \tag{4}$$

In summary, the geometric parameters of single multi-segment which labeled in figure 3 (c) can be summed up as Table I. Besides, the material of sliding spring used in this robot is 65Mn with a size 130 mm × 8 mm ×0.4 mm in length, wideness, thickness.

TABLE I. PARAMETERS VALUE OF MULTI-SEGMENT UNIT

Element	Parameters of multi-segment unit		
	Value	Element	Value
h	6.3 mm	b	6 mm
d	1.5 mm	α_0	7 °
w	10 mm	n	9
W	14 mm	h_0	3.4 mm

n refers to the number of multi-segment units in total

D. Design of hand fixing plate

We designed a plate which uses Velcro to constrain it on the back of hand, and there are two thrust bearings to connect this plate with the end of the multi-segment mechanism. That allows the wrist to rotate without changing the pose of multi-segment mechanism. The wrist rotation model [9] is built in Figure 4. It represents the wrist's cross section, in which the blue square represents the thrust bearing, and the horizontal line is the fixed plate.

Once a linear motor moves forward and another moves inversely, it will form a height difference between the two ends of the multi-segment mechanism, that will consequently lead to rotation in z axis. In Figure 4, the dashed line is the baseline before bending, h is the height of change, R is the geometric radius of the bend, and θ is the angle of the bend. L is the distance between the center of bearing and rotation center of wrist. α_0 is the designed angle between multi-segment units. According to geometrical knowledge, the following formats can be induced.

$$S_1 = \left(\frac{l}{2\tan\frac{\theta}{2}} + H \right) \cdot \theta - l \tag{5}$$

$$S_2 = 1 - \left(\frac{1}{2\tan\left(\frac{\alpha_0 \cdot n}{2}\right)} - h \right) \cdot n\alpha_0 \qquad (6)$$

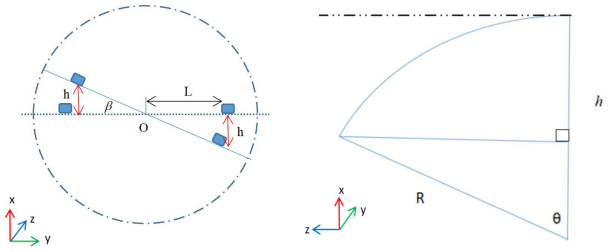

Figure 4. Wrist model of rotation

C. Fabrication and control system

Most of the rigid components are 3D printed by a 3D printer (JGAURORA, Shenzhen Aurora Technology co., LTD) of PLA material. As previous narrative, the bearing base with two vertical placed bearings connects the motor and sliding spring, these two bearings provide rotation DOF in Y-O-Z and X-O-Y plane, respectively. The actuators (ACTUONIX L12-50-210-12-l, Firgelli Technology Inc, Canada) are installed on a 3D printed arm stand that are fixed on the forearm by Velcro. The fabricated exoskeleton prototype is shown in Figure 5. An Arduino Mega-2560 controller board is integrated with the exoskeleton to receive motion signal from the upper system, then converts it into voltage signal to actuate the linear motors.

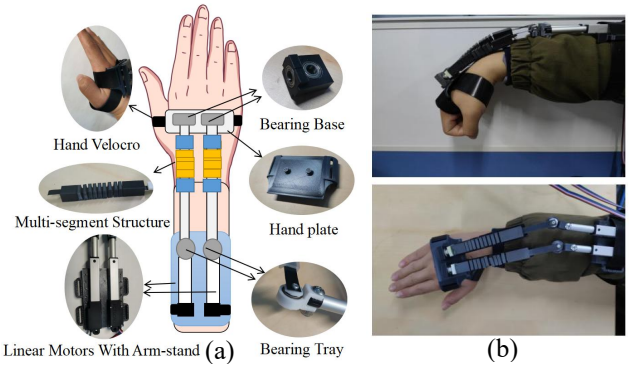

Figure 5. Overview of the wrist exoskeleton

From hand to forearm, there are hand plate with Velcro to tie on hand, bearing bases with two vertical placed bearings, multi-segment mechanism limiting the deformation of sling spring, bearing trays as a joint and using arm-stand to fix linear motor on the forearm. Notably, the integrated system without battery only weights 248 g.

III. EXPERIMENTS AND RESULTS

To test the feasibility and performance of this design, we conducted three experiments. Including range of motion and trajectory tests, bearing force range of multi-segment mechanism, human equipped rehabilitation training assessment.

A. Range of motion and trajectory test

We conducted the following experiments to measure the range of motion in several rehabilitation movements and trajectory of flexion and extension. The exoskeleton was assembled according to Figure 5, and the motors were stuck on the arm stand that was nailed on a fixed horizontal board. The first block of this mechanism was clamped in a vice stand to stimulate the situation that equipped on human's extremity, the setup is shown in Figure 6 (a). During the flexion/extension experiment, a camera (Canon 200D, Canon, Japanese) was mounted on a tripod to the same height of the mechanism to record high-quality videos of experiments process. Besides, a graph paper was posted behind as a preference of trajectory's coordinate as Figure 6 (b). When testing the feasible angles of radial deviation/ulnar deviation, the camera was mounted above the mechanism as Figure 6 (c). The camera was placed diagonally below the platform when testing the rotation of this exoskeleton. The camera was placed diagonally below the platform when testing the rotation of this exoskeleton as Figure 6 (d).

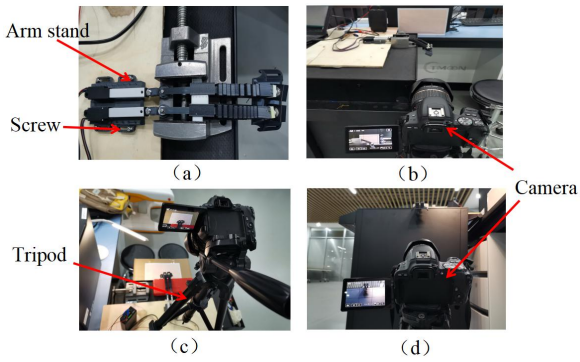

Figure 6. Experiment setup for range of motion and trajectory

After setting up the experiment system for each DOF, we controlled the linear motors executing displacement combinations as Figure 2 to carry out different movements. The test was repeated three times. We picked up 3 representative points from the multi-segment mechanism, then used the average value of these three tests to draw the trajectory curve as Figure 7. The three points are the first block's upper-right point, the fourth block's upper-right point and the last block ' s upper-right point. As a result, the trajectories are smooth and stable.

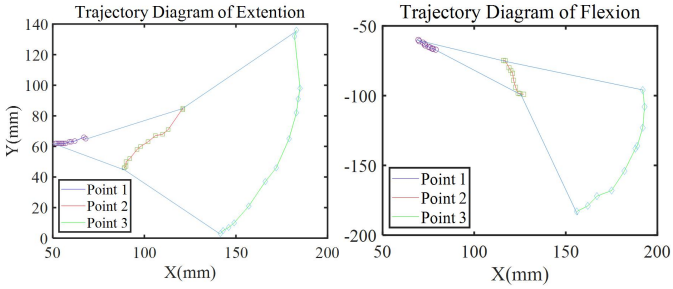

Figure 7. Trajectory of multi-segment mechanism

By analyzing the videos in each 10 frames, we get the range of motion for flexion/extension are 71.2° and 66.4°, in radial deviation/ulnar deviation the numbers are 24.5 ° and 19.4 ° , for pronation/supination, the ranges of motion are 48.3° and 50.1°, respectively. Therefore, it can approximately meets the wrist rehabilitation requirements in II.A.

B. Force range of multi-segment mechanism

To test the force that can be provided by single

multi-segment mechanism and its mechanical characteristics, we carried out this experiment as Figure 8, in which the multi-segment mechanism was clapped by a vice stand that fixed horizontally on a platform. The first block of multi-segment mechanism and the front part of linear motor was clapped by the vice stand to simulate the maximum linear displacement condition. A 3D-printed cylinder was fixed under a force sensor (Model THL-1, Bengbu, China) to bear the force from multi-segment mechanism. In this experiment, the multi-segment mechanism maintained the gesture of flexion or extension, and the lifting platform's lifting forced the end of the multi-segment mechanism to raise to the same height as its first block, then the platform went down until it did not contact with the mechanism. The output of the sensor was recorded in each 3 mm cylinder displacement and the test was repeated three times.

As shown in Figure 9, the utmost force provided by one mechanism were 7.45 N and 5.84 N for flexion and extension, the corresponding torque were 0.67Nm and 0.53Nm, respectively. Theoretically, the exoskeleton can generate torques about 1.34Nm and 1.06Nm for flexion and extension, respectively, that meets the rehabilitation requirements well. Moreover, the loading and unloading curves are even and stable.

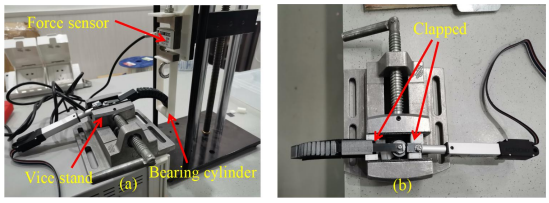

Figure 8. Output force measurement experimental setup

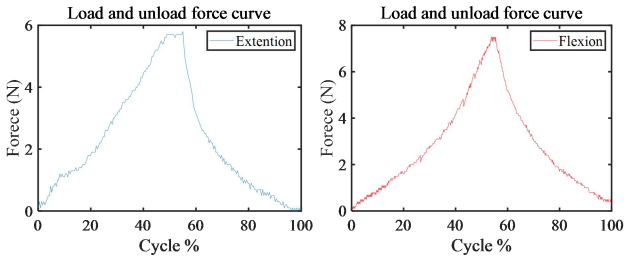

Figure 9. Loading and unloading curve

C. Promotions comparison

Compared with the former version exoskeleton, multi-segment mechanism has several promotions as listed.

TABLE II. PARAMETERS VALUE OF MULTI-SEGMENT UNIT

Characteristic	Different version of exoskeleton	
	Only sliding spring	With multi-segment
DOF	two	three
Range of stroke	100 mm	50 mm
Weight with motors	288g	248g
Motors expenditure	2×129 USD	2×99 USD
Trajectory	Unstable and uncontrollable	Stable and controllable
Maximum Force/Torque	10.24 N/0.92Nm	14.9N/1.34Nm

The main promotions are one more DOF for rehabilitation training, namely pronation /supination, which is more applicable for real rehabilitation, and 50% reduction in the displacement requirements of linear motors that considerably reduces the cost and weight of the exoskeleton. Moreover, the rigid-soft combined structure provides bigger torques that meets the requirement of wrist rehabilitation.

IV. Conclusion

In this study, we designed a wrist exoskeleton using a multi-segment mechanism to realize rehabilitation movements in three DOFs. This exoskeleton can be used in CPM or active rehabilitation depending on the control strategy. It has three significant advantages compared with the one only using sliding spring. Firstly, this device can realize soft-rigid combined rehabilitation in three DOFs, which is more applicable for real human rehabilitation. Secondly, it can achieve larger range of motion within the same linear stroke. That makes it more compact and lighter in hardware with a lower cost. Moreover, it has a certain rehabilitation trajectory which can not only prevent secondary injury but also provide stable and safe rehabilitation training.

However, applications on human body would have impact on the actual performance of the exoskeleton. Therefore, human equipped experiments should be conducted in the future to study the range of motions, force characteristics, etc. The trajectory experiments should also be repeated by using more high-precision instruments. For further researches, the parameters of each multi-segment blocks can be customized for specific users to realize optimal performance, such as more harmonious trajectory and better force characteristics.

References

[1] Gupta, Abhishek, et al. "Design, Control and Performance of RiceWrist: A Force Feedback Wrist Exoskeleton for Rehabilitation and Training," The International Journal of Robotics Research 27.2 (2008): 233-251.

[2] T. Higuma, K. Kiguchi, and J. Arata, "Low-Profifile Two-Degree-of-Freedom Wrist Exoskeleton Device Using Multiple Spring Blades," IEEE Robot. Autom. Lett., vol. 3, no. 1, pp. 305–311, Jan. 2018, doi: 10.1109/LRA.2017.2739802.

[3] H. Choi, B. B. Kang, B.-K. Jung, and K.-J. Cho, "Exo-Wrist: A Soft Tendon-Driven Wrist-Wearable Robot With Active Anchor for Dart-Throwing Motion in Hemiplegic Patients," IEEE Robot. Autom. Lett., vol. 4, no. 4, pp. 4499–4506, Oct. 2019, doi: 10.1109/LRA.2019.2931607.

[4] Zhu, S. , et al. "Finger Exoskeleton for Rehabilitation of Finger Extension and Flexion by Multi-Segment Mechanism," Journal of Xi'an Jiaotong University(2018).

[5] M. Li et al., "Attention-controlled assistive wrist rehabilitation using a low-cost EEG Sensor," IEEE Sensors J., vol. 19, no. 15, pp. 6497–6507, Aug. 2019, doi: 10.1109/JSEN.2019.2910318.

[6] Ryu, J. , et al. "Functional ranges of motion of the wrist joint," The Journal Of Hand Surgery 16.3(1991):409-419.

[7] Lannin, N. A., Cusick, A., McCluskey, A. & Herbert, R. D. "Effects of Splinting on Wrist Contracture After Stroke: A Randomized Controlled Trial," Stroke 38, 111–116 (2007).

[8] Ruby, L. K. , et al. "Relative motion of selected carpal bones: A kinematic analysis of the normal wrist," Journal of Hand Surgery 13.1(1988):1-10.

[9] H. Okada, M. Ae, N. Fujii, and Y. Morioka, "Body segment inertia properties of Japanese elderly," (in Japanese), Soc. Biomechanisms Jpn.,vol. 13, pp. 125–139, 1996.